Structural Engineering and Mechanics, *Vol. 69, No. 2 (2019) 163-175*
DOI: https://doi.org/10.12989/sem.2019.69.2.163

Effective CFRP retrofit strategy for flexural deficient RC beams

Nawal Kishor Banjara*[1,2] and K. Ramanjaneyulu[1,2]

[1]*Academy of Scientific and Innovative Research, CSIR Campus, Taramani, Chennai-600113, India*
[2]*CSIR-Structural Engineering Research Centre, CSIR Campus, Taramani, Chennai-600113, India*

(Received May 14, 2018, Revised November 27, 2018, Accepted December 1, 2018)

Abstract. Structural deterioration arises due to aging, environmental effects, deficiencies during design and construction phase, and overloading. Experimental and numerical investigations are carried out in this study to evaluate the performance of control and flexural deficient reinforced concrete (RC) beams under monotonic loading. Three levels of flexural deficiency are considered in this study. After confirming load carrying capacities of control and flexural deficient beams, the flexural deficient RC beams are strengthened with carbon fibre reinforced polymer (CFRP) fabric. CFRP strengthened RC beams are tested under monotonic loading and compared with the performance of control specimen. Further, non-linear finite element analyses are also carried out to evaluate the flexural performance of control, deficient and CFRP strengthened flexural deficient RC beams. There is good correlation between results of experimental and numerical investigations. Numerical approach presented in this study can be adopted for assessing the adequacy of CFRP retrofit measure.

Keywords: flexural deficient; monotonic loading; CFRP strengthening; experimental investigation; numerical simulation

1. Introduction

Structural failure refers to the loss of structural integrity and load carrying capacity. When a material is stressed to its strength limit, failure gets initiated with associated excessive deformations and fracture. A structure can become deficient in flexure depending on structural and loading conditions. Reinforced concrete structures are often affected by corrosion of reinforcement bars. The corrosion damage may reduce the flexural capacity of reinforced concrete structural elements. Repair and rehabilitation of these deficient structures/structural components is gaining popularity.

The behavior of reinforced concrete beams strengthened with various types of fiber reinforced polymer (FRP) laminates were experimentally investigated by Grace *et al.* (1999). It was concluded that, in addition to the longitudinal layers, the fibers oriented in the vertical direction forming a U-shape around the beam cross section significantly reduce beam deflections and increase beam load carrying capacity. Ekenel *et al.* (2006) carried out a study on the flexural strengthening of reinforced concrete (RC) beams with two FRP systems. The results showed that use of anchor spikes in fabric strengthening increase ultimate strength, and mechanical fasteners can be an alternative to epoxy bonded pre-cured laminate systems. Six reinforced concrete beams strengthened in flexure using carbon-fibre-reinforced polymer (CFRP) laminates subjected to different sustaining loads were tested by Wenei and Guo, (2006). Results of the study had shown that sustaining load levels at the time of strengthening have important influence on the ultimate strength of strengthened reinforced concrete beams. Lim (2009) investigated the effectiveness of flexural strengthening of beams reinforced with near-surface mounted (NSM) and externally bonded reinforcing (EBR) CFRP strips. It was found that the flexural stiffness and strength of the beams reinforced with NSM and EBR strips were significantly improved compared with the beams strengthened only with NSM CFRP strip.

Laboratory tests on concrete beams strengthened with epoxy bonded CFRP plates were carried out by Rusinowski and Täljsten (2009). CFRP sheets were wrapped to localize the failure initiation. Concrete cracking as well as debonding initiation and propagation was observed with help of high speed camera. Dias and Barros (2011) investigated the effectiveness of five NSM shear strengthening configurations (three CFRP orientations and two levels of CFRP percentage) applied to T-section RC beams with steel stirrups percentage of 0.10% and 0.17%. The predicted values of the CFRP contribution for the shear resistance were found to be 75% of that registered experimentally. The experimental investigations on the flexural strengthening of reinforced concrete beams by CFRP laminates affixed to the tensile soffit of the beams by epoxy adhesive was carried out by Ahmed *et al.* (2011). A total of six reinforced concrete beams having different degrees of strengthening were tested to failure under transverse bending. The increase in ultimate strength provided by the bonded carbon fiber was assessed by varying the layers of composite laminates. De-bonding of CFRP laminates from concrete surface was observed in the case of multi-layer strengthening of beam.

The experimental research conducted by Dong *et al.* (2012) on RC beams strengthened with FRP sheets showed

*Corresponding author, Scientist
E-mail: nawal1234@gmail.com, nawalkishor@serc.res.in

ISSN: 1225-4568 (Print), 1598-6217 (Online)

significant enhancement in ultimate strength and fatigue resistance. The experimental tests were conducted on RC beams retrofitted by unconventionally arranged CFRP strips and on a reference (not retrofitted) one by Bocciarelli *et al.* (2013). Diagonal CFRP strips were applied on the lateral faces of the specimens and connected to the longitudinal ones in order to improve the anchorage length of the latter. Haddad *et al.* (2013) investigated the potential of using advanced composite materials in repairing deficient reinforced concrete prototype damaged beams. The results confirmed that FRP composites not only enhanced the load carrying capacity but also improved deflection characteristics, stiffness, toughness, profitability index, crack resistance, performance factor, and FRP composites strain. An experimental and analytical study to investigate the flexural behaviour of reinforced concrete beams strengthened using carbon-fibre reinforced polymer (CFRP) laminate was carried out by Boukhezar *et al.* (2013). The experimental and analytical results indicated that the flexural capacity and stiffness of strengthened and repaired beams using CFRP laminates were increased compared with those of control beams.

The experimental investigations carried out by El-Gamal *et al.* (2016) on reinforced concrete (RC) beams strengthened with NSM glass and carbon fiber reinforced polymers showed increase in the ultimate load carrying capacity between 31 and 133% depending on amount and type of FRP used, compared with the reference beams. Afefy *et al.* (2016) conducted experimental and analytical studies on the flexural behaviour of fully composite steel-concrete I-girders strengthened by externally bonded carbon fiber reinforced polymer (EB-CFRP) sheets. An analytical design procedure was proposed in order to obtain the moment of resistance of the composite girders. Peng *et al.* (2016) studied the behaviour of seven RC beams (two regular and five beams strengthened with externally bonded non-prestressed and prestressed CFRP plates) to examine the effects of different strengthening methods on the flexural fatigue performance of the beams. It was evident from the experimental results that strengthening with prestressed CFRP plates significantly enhanced the monotonic and fatigue performances of reinforced concrete beams. Zhang and Kanakubo (2016) carried out experimental investigations on externally bonded CFRP plate debonding behaviour. It was reported that the performance of structure strengthened with CFRP plate depends on shear bond strength of the interface. Saribiyik and Caglar (2016) manufactured RC beam specimens with insufficient shear and tensile reinforcement and low strength concrete. The performance of the RC specimens strengthened with CFRP and Glass Fibre Reinforced Polymer (GFRP) composites were examined. It was concluded that although the flexural and shear strengths of the RC beams strengthened with GFRP composites were lower than those of beams reinforced with CFRP, their ductility and energy absorption capacities were very high. Investigations on the improvement in the flexural capacity and cracking resistance of continuous steel-concrete composite beams strengthened with CFRP laminates at the hogging moment regions was carried out by El-Zohairy *et al.* (2017). The experimental findings were used to develop and validate a finite element (FE) model to simulate the nonlinear flexural performance of strengthened beams as well as plain beams. The flexural performance of RC beams externally bonded with CFRP grid-reinforced engineered cementitious composite (ECC) matrix was carried out by Yang *et al.* (2018). The flexural strengthening configuration using the epoxy adhesive to bond prefabricated CFRP grid-reinforced ECC plate proved to be the most efficient solution.

From the review of the existing literature, it is found that though many discrete research works were carried out on response of deficient RC structural components, the following issues are still open and needs adequate attention: (i) Experimental investigations on the behaviour of RC beams with different levels of flexural deficiency, (ii) Influence of CFRP strengthening layers on the load carrying capacity and performance and (iii) numerical models to evaluate the performance of deficient and CFRP strengthened flexural members. In view of this, in the present study, experimental and numerical investigations are carried out to understand the behaviour of RC beams with different levels of flexural deficiency and CFRP strengthened deficient RC beams under monotonic loading.

2. Experimental investigations on flexural deficient RC beams

To investigate the behaviour of control and flexural deficient reinforced concrete (RC) rectangular beams, experimental investigations are carried out. Three control (C) beams of rectangular cross section are designed for balanced reinforced condition as per IS 456 (2000) and six flexural deficient beams compared to the control beams are designed and cast. Three levels of flexural deficiency, viz., 20%, 30% and 50% are considered in this study for design of flexural deficient RC beams and the beams with these deficiencies are respectively designated as FD1, FD2 and FD3. The overall length of the RC beam is chosen as 1800 mm with cross section dimensions of 150 mm×200 mm as shown in Fig. 1(a). The effective span of the beam is 1500 mm. A clear cover of 25 mm is adopted. The reinforcement details of control (without deficiency) and flexural deficient FD1 (20%), FD2 (30%) and FD3 (50%) RC beams are shown in Fig. 1(b). RC beams are cast using designed concrete mix having characteristic compressive strength of 40 MPa. Ordinary Portland cement (OPC) of 53 grade, natural sand, and coarse aggregates of size 10 mm/20 mm are proportioned in the ratio of 1:2.25:2.35 respectively with water-to-cement ratio of 0.5, for the desired concrete mix. In addition to the test beams, six cubes of size 150 mm×150 mm×150 mm and six cylinders of size 150 mm×300 mm, are cast to evaluate material parameters of concrete. From the material test data, average values of compressive strength of six cubes, modulus of elasticity of three cylinders and split tensile strength of three cylinders for the concrete used in the present study are found to be 44.7 MPa, 31,500 MPa and 3.2 MPa, respectively. For

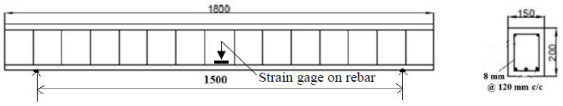

(a) Geometry of RC beams

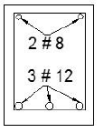

(i) Control

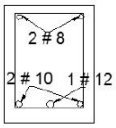

(ii) FD1 (20%)

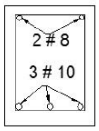

(iii) FD2 (30%)

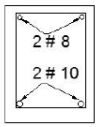

(iv) FD3 (50%)

Note: 2#8 - 2 numbers of 8 mm diameter bar (typical)

(b) Reinforcement details of control and flexural deficient RC beams

Fig. 1 Cross sectional and reinforcement details of the control and flexural deficient RC beams considered in this study

(i)

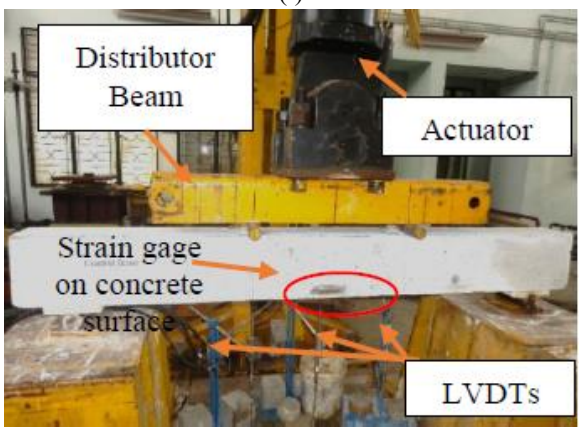

(ii)

Fig. 2(a) (i) Strain gages pasted on reinforcement bar and (ii) actual test set up

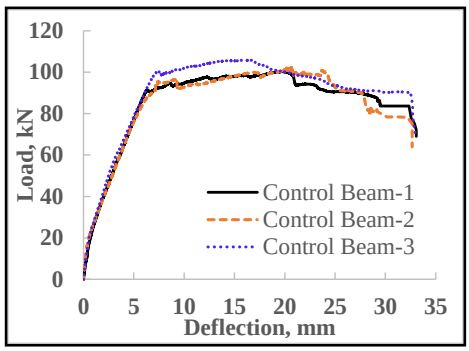

(i) Control

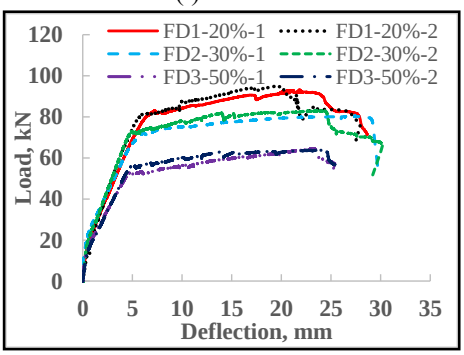

(ii) flexural deficient

Fig. 2(b) Load versus displacement curves of (i) control beam and (ii) flexural deficient (FD1, FD2 and FD3) RC beams

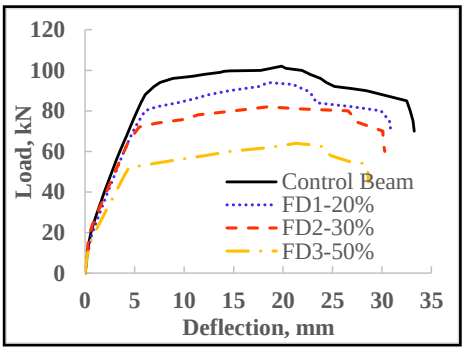

Fig. 2(c) Average load displacement curves of control and flexural deficient RC beams

evaluating fracture energy, three concrete prism specimens of size 100 mm×100 mm×500 mm are cast. After curing period, a centre notch of 5 mm wide and 20 mm deep is created in prism specimens.

Notched prisms are tested under three-point bending. Average fracture energy is evaluated and is found to be 126 N/m, and the same is used for numerical simulations. Electrical resistance strain gages are affixed on reinforcement bars and on concrete surface, to obtain strain in the reinforcement and concrete during testing. One strain gauge of 5 mm gauge length and 120-ohm resistance is pasted at centre of all the beam bottom reinforcement bars, as shown in Fig. 2(a). On the concrete surface, two strain gauges of 60 mm gauge length are pasted on front and back faces, at centre of span, at 25 mm from the soffit of the beam, as shown in Fig. 2(a), before starting the test, in order to get complimentary measurement for the strain to be measured on the reinforcement bars, as there is a chance for the strain gages on reinforcement bars getting damaged during concreting. Four-point bending tests are carried out under monotonic loading using hydraulic actuator of 500 kN capacity and stroke length of ±125 mm. Test setup used for experimental investigations is shown in Fig. 2(a). Load deflection curves for each specimen in each group, namely

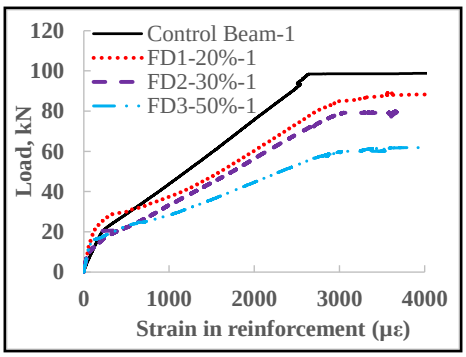

(i)

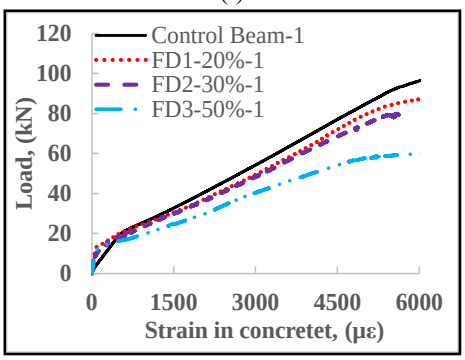

(ii)

Fig. 2(d) (i) Load versus strain in reinforcement and (ii) load versus strain in concrete

control and flexural deficient RC beams with different levels of deficiency (FD1, FD2 and FD3), are shown in Fig. 2(b). Fig. 2(c) shows comparative average load deflection graphs for different groups for bringing out the effect of deficiencies on load carrying capacity. Average load carrying capacity of control, FD1, FD2 and FD3 beams are found to be 102 kN, 92 kN, 79 kN and 63 kN, respectively. Load carrying capacity of flexural deficient RC beam is reduced with respect to control beam due to reduction in the moment carrying capacity of the beam with flexural deficiency.

Load versus strain in reinforcement and concrete for typical specimen-1 of control and flexural deficient (FD1, FD2 and FD3) RC beams are shown in Fig. 2(d). As the clear cover adopted is 25 mm and the diameter of the stirrup is 8 mm, the measurement of strain on reinforcement bars is around 35 mm from the soffit of the beam. In view of the difference in the distances of measurement of strain from the soffit of the beam, at a given load level, strain value recorded by the strain gages affixed on concrete surface at 25 mm from the soffit is higher than the strain value recorded by the strain gage affixed on the reinforcement bar, as can be seen from Fig. 2(d).

Details, such as ultimate load carrying capacity, and deflections at yielding and ultimate of RC beams are presented in Table 1. In the beams tested in this study, flexural cracks are developed at first. With increase in load, flexural cracks are propagated and beams are failed with excessive deformation. Failure patterns for all the specimens of different categories (control and flexural deficient) of RC beams are shown in Figs. 3(a)-3(d).

Table 1 Behaviour of RC beams at yielding and ultimate load

Specimen ID	At yielding		At ultimate Load				D_R	Energy absorption (E) (kN-mm)		
			Load, P_u (kN)							
	P_y (kN)	δ_y (mm)	P_{ui}	P_{ua}	% Reduction in P_u	δ_u (mm)	$(\frac{\delta u}{\delta y})$	E_i	E_a	% Reduction in E
Control-0%-1	93.63	7.35	97.62			15.46	2.10	3174		
Control-0%-2	96.54	7.62	101.74	102	-	16.15	2.12	3477	3466	-
Control-0%-3	100.12	7.84	105.36			16.36	2.08	3748		
FD1-20%-1	85.23	7.25	90.54			16.62	2.29	2818		
				92	9.80				2783	19.70
FD1-20%-2	87.05	7.38	93.12			17.33	2.34	2747		
FD2-30%-1	73.63	7.22	78.03			15.85	2.19	2301		
				79	22.60				2393	30.95
FD2-30%-2	75.45	7.15	80.36			16.44	2.30	2484		
FD3-50%-1	55.78	7.65	61.28			12.32	1.61	1812		
				63	38.20				1903	45.10
FD3-50%-2	58.16	8.17	64.05			13.76	1.68	1993		

Note: -P_y -load at yielding; P_{ui} -ultimate load of individual specimen; P_{ua} -average ultimate load; δ_y -deflection at yielding; δ_u -deflection at ultimate load; D_R -ductility ratio; E_i -energy absorption of individual specimens; E_a -average energy absorption

Based on the results of experimental investigations carried out in this study on nine RC beams (three control and six flexural deficient RC beams), the plot of % reduction in ultimate load versus % flexural deficiency is plotted as shown in Fig. 4. Trend line of % reduction in ultimate load with % flexural deficiency is also obtained. This trend line can be used for estimation of % reduction in ultimate load of flexural deficient RC beams of any deficiency level with reference to control beam (without any flexural deficiency), within the bounds of experimental results (i.e., 20-50% flexural deficiency). This would help in deciding on the level of strengthening required. Further, from the results presented in Table 1, it may be noted that % reduction in energy absorption with respect to that of control beam specimen is proportional to the flexural deficiency.

From Table 1 and Fig. 4, it is observed that load carrying capacity of critical deficient RC beam (FD3) is reduced by around 40% with respect to control beam. It is found that control beams are failed in combined shear and flexural failure. Flexural deficient RC beams are failed in flexural failure. After confirming the load carrying capacity and behaviour of RC beams under monotonic loading, RC beams are taken up for strengthening with CFRP fabric. Analytical formulations are developed for arriving at the required number of CFRP fabric layers for strengthening.

3. Analytical formulations for designing number of CFRP layers required for strengthening of flexural deficient RC beams

First, analytically, flexural capacity of the strengthened beam is evaluated. The nominal flexural strength of RC beam strengthened by means of externally bonded CFRP

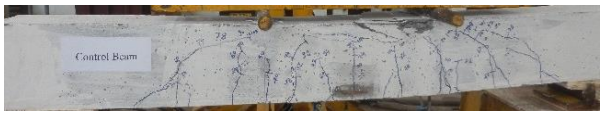

(i) Specimen-1

(ii) Specimen-2

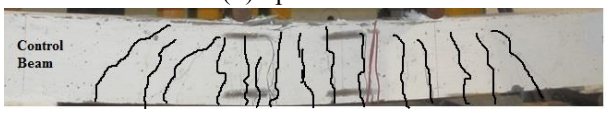

(iii) Specimen-3

(a) Control beam

(i) Specimen-1

(ii) Specimen-2

(b) FD1

(i) Specimen-1

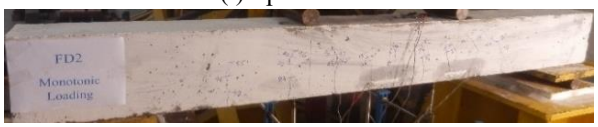

(ii) Specimen-2

(c) FD2

(i) Specimen-1

(ii) Specimen-2

(d) FD3

Fig. 3 Failure patterns of control and flexural deficient (FD1, FD2 and FD3) RC beams

fabric can be evaluated as a sum of the flexural resistance contribution of reinforcement and bonded fabric (ACI 440 2008). Fig. 5 shows the idealized forces, strains and corresponding stresses within a concrete beam resisting an applied moment. The analytical procedure involves assuming depth of neutral axis (c) at first and followed by calculating the strain in steel and composite matrix based on strain compatibility; calculating the associated stress level in the respective material; and checking the internal force

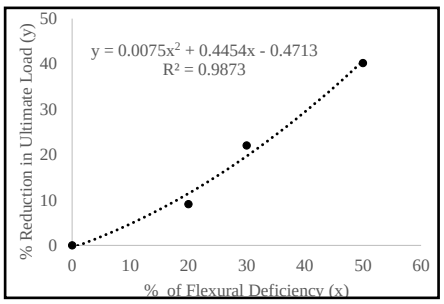

Fig. 4 Effect of level of flexural deficiency on the ultimate load

equilibrium. If the internal force resultants do not equilibrate, the depth to the neutral axis should be revised and the procedure is to be repeated. Thus, steps to be followed to arrive at the number of CFRP fabric layers required for strengthening of flexural deficient RC beams are given below. For any assumed depth to the neutral axis (c), the strain level in the CFRP reinforcement is computed from Eq. (1).

$$\varepsilon_{fe} = \varepsilon_c \left(\frac{d_f - c}{c} \right) - \varepsilon_{bi} \tag{1}$$

where ε_c is ultimate strain in concrete, d_f is the total depth of flexural member, ε_{bi} is the initial substrate strain.

The effective stress (f_{fe}) level in the CFRP reinforcement is the maximum level of stress that can be developed in the CFRP reinforcement before flexural failure of the section. This effective stress level in the CFRP reinforcement can be found from Eq. (2).

$$f_{fe} = E_f \varepsilon_{fe} \tag{2}$$

where E_f is the elastic modulus of CFRP and ε_{fe} is the strain in CFRP.

The stress in the steel as given in equation (3) can be determined from the strain level in the steel using its stress-strain curve.

$$f_{st} = E_s \varepsilon_s \leq f_y \tag{3}$$

After determining the strain and stress level in the CFRP reinforcement and steel reinforcement, the compression and tensile forces are evaluated based on the force distribution shown in Fig. 5 as follows

$$F_c = \beta_1 c \alpha_1 f_c' b \tag{4}$$

$$F_T = A_s f_s + A_f f_{fe} \tag{5}$$

where A_s is area of steel reinforcement, f_s tensile stress of reinforcement, A_f cross section area of CFRP, f_{fe} is the equivalent stress in CFRP, α_1 and β_1 are the stress block constants (0.85 and 0.75, respectively). Area of the externally bonded CFRP reinforcement is expressed as, $A_f = n\, t_f w_f$, where n is the number of CFRP layers, t_f is thickness of CFRP material and w_f is the width of CFRP matrix.

F_c should be equal to F_T for ensuring force equilibrium. If force equilibrium is not established, a revised value for

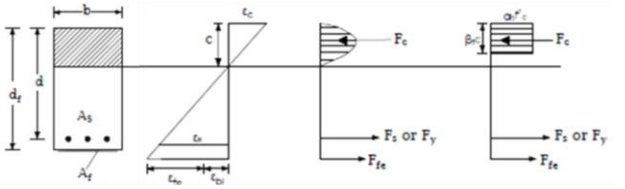

Fig. 5 Internal strain and stress distribution for a rectangular section under flexure at ultimate (ACI 440)

the depth (c) of neutral axis is then assumed based on the magnitudes of F_c and F_T. The above procedure is repeated till the force equilibrium is established. Once the force equilibrium is established for the neutral axis depth (c), strain (ε_{fe}) and stress (f_{fe}) in CFRP are evaluated.

Total force at ultimate due to steel reinforcement and CFRP fabric are evaluated using Eq. (6)

$$F_T = F_{st} + F_{fe} \tag{6}$$

where F_T is total force, F_{st} is load taken by steel reinforcement and F_{fe} is the load taken by externally bonded CFRP fabric layer.

The moment carrying capacity of CFRP strengthened deficient RC beam is evaluated using reduction factor of 0.85 for the contribution of CFRP reinforcement as given in Eq. (7)

$$M = A_s f_s \left(d - \frac{\beta_1 c}{2}\right) + 0.85\ A_f\ f_{fe} \left(d_f - \frac{\beta_1 c}{2}\right) \tag{7}$$

In this study, using above analytical procedure, number of CFRP fabric layers required are evaluated. Based on Eqs. (1) to (7), a single layer of CFRP fabric is found to be sufficient for the moment carrying capacity of flexural deficient RC beams FD1 and FD2 to reach up to that of the control beam but for critical deficient FD3 beam (with 50% flexural deficiency), single layer is found to be not sufficient. Using analytical expressions presented above, it is found that the load carrying capacity of critical flexural deficient RC beam (FD3) strengthened with single CFRP layer is around 84 kN. For FD3 beam strengthened with two CFRP layers, the load carrying capacity is found to be 105 kN. It is understood that two number of CFRP layers are required to bring the load carrying capacity of critical flexural deficient RC beam (FD3), on par with that of control beam. Experimental study is carried out to demonstrate the efficacy of CFRP strengthened RC beams using single layer of CFRP fabric.

4. Experimental investigations on CFRP strengthened flexural deficient RC beams (designated as SFD1, SFD2 and SFD3)

Before starting strengthening, surface of the beam is prepared properly and epoxy adhesive is mixed properly as shown in Figs. 6(a) and 6(b). Sikadur-330 is used as adhesive material. CFRP fabric (Sikawrap 450C) which is used for flexural strengthening of RC beams in this study is shown in Fig. 6(c). Material properties of Sikadur-330 and Sikawrap 450C are given in Table 2. Strengthening of

Table 2 Material properties of epoxy and CFRP

Properties	Material	
	Epoxy (Sikadur -330)	CFRP Fabric (Sikawrap 450C)
Elastic modulus (MPa)	3800	2.3×10^5
Tensile Strength (MPa)	30	4000
Density (kg/m^3)	1200	1820
Poisson's ratio	0.21	0.10
% elongation	0.9	1.7
Thickness	0.8-1.0	0.255 mm

(a)

(b)

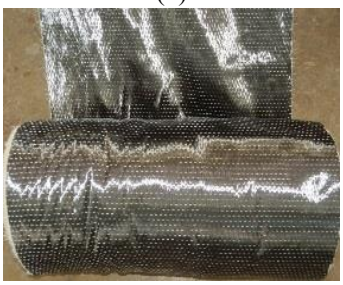

(c)

(d)

Fig. 6(a) Surface preparation, (b) mixing of adhesive material, (c) view of CFRP fabric and (d) CFRP strengthened beams

flexural deficient (FD1, FD2 and FD3) beams is carried out using one layer of CFRP fabric as shown in Fig. 6(d) and are designated respectively as SFD1, SFD2 and SFD3.

After curing, CFRP strengthened beams (designated as SFD1, SFD2 and SFD3) are tested under monotonic loading. Individual load versus deflection curves of all the specimens of different categories of CFRP strengthened

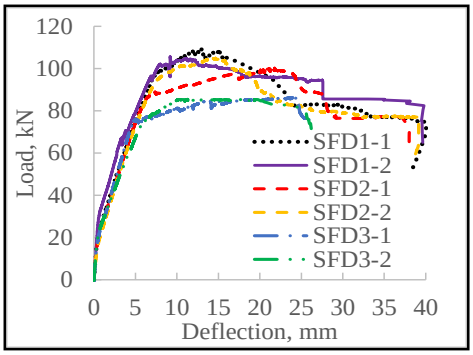

(a) CFRP Strengthened beams

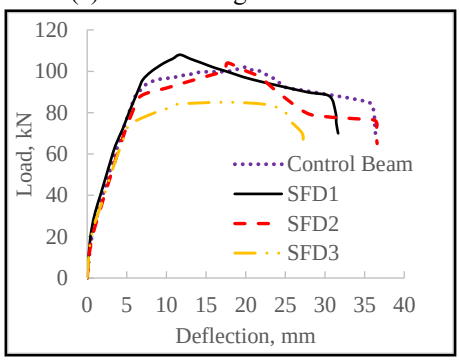

(b) Comparison

Fig. 7 Load versus deflection curves of CFRP strengthened flexural deficient RC beams

(i) Specimen-1

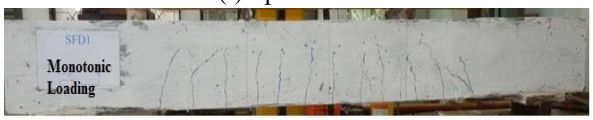

(ii) Specimen-2

(a) SFD1

(i) Specimen-1

(ii) Specimen-2

(b) SFD2

(i) Specimen-1

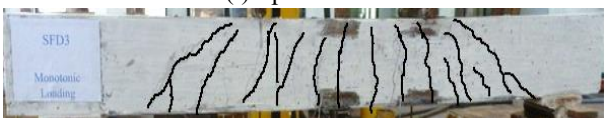

(ii) Specimen-2

(c) SFD3

Fig. 8 Typical failure patterns of CFRP strengthened deficient RC beams, (a) SFD1, (b) SFD2 and (c) SFD3

flexural deficient RC beams (SFD1, SFD2 and SFD3) are shown in Fig. 7(a). Fig. 7(b) shows average load deflection graphs of control and strengthened flexural deficient RC beams (SFD1, SFD2 and SFD3). Strengthened RC beams are failed due to yielding of reinforcement and fracture of the CFRP fabric. Delamination of the CFRP fabric was not observed during the testing of the specimens. Failure patterns for all the specimens of different categories of CFRP strengthened (SFD1, SFD2 and SFD3) RC beams are shown in Figs. 8(a) to 8(c) respectively.

It is found that load carrying capacity of strengthened flexural deficient beams SFD1 and SFD2 with one layer of CFRP fabric, reached to the same level as that of control beam but load carrying capacity of strengthened critical flexural deficient RC beam SFD3 with one layer of CFRP fabric, reached around 80% of that of control beam. Hence, it is observed that for strengthening of flexural deficient RC beams, FD1 and FD2, one layer of CFRP fabric is found to be sufficient. However, it is noted that one layer of CFRP fabric is found to be not sufficient for FD3 specimen to gain strength equal to that of control specimen.

Fig. 9(a) shows load versus deflection curves of typical specimen-1 of control beam, flexural deficient (FD3) and deficient RC beam strengthened with one layer of CFRP fabric (SFD3). Strain in reinforcement bar and strain in concrete for typical specimen-1 of CFRP strengthened critical flexural deficient beam SFD3 are shown in Figs. 9(b)-9(c) respectively. At a given load level, strain value recorded by the strain gages affixed on concrete surface at 25 mm from the soffit of the beam is higher than the strain value recorded by the strain gage affixed on the reinforcement bar at 35 mm from soffit of the beam, as can be seen from Figs. 9(b) and (c). It is found that load carrying capacity of CFRP strengthened flexural deficient RC beam -SFD3 is increased by around 37% compared with that of flexural deficient (FD3) RC beam. Also, the strain in SFD3 at the same load level is found to be lesser than deficient RC beam FD3. From the analytical and experimental studies, it is observed that one layer of CFRP fabric has improved load carrying capacity of the 50% flexural deficient beam -FD3 by around 37%. But, still load carrying capacity of SFD3 has not reached the level equal to that of control beam. Details such as ultimate load carrying capacity, deflection at yielding and ultimate, ductility ratio and energy absorption of strengthened flexural deficient RC beams are presented in Table 3.

Though the numerical modelling cannot be claimed as substitute for experimental investigations, experimentally validated numerical models can complement the experimental investigations and can effectively be used for further evaluation and parametric study. Hence, in this study, numerical models are developed to evaluate the behaviour of flexural deficient and deficient beams strengthened with one layer of CFRP fabric. The validated models are further used to evaluate the behaviour of critical

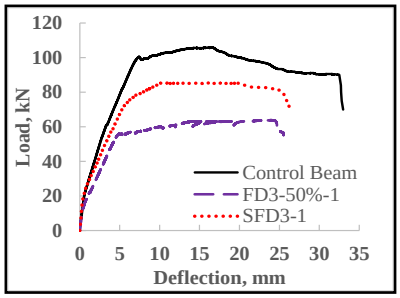

(a)

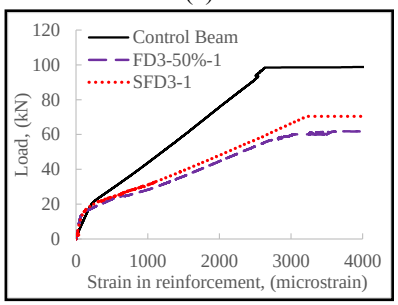

(b)

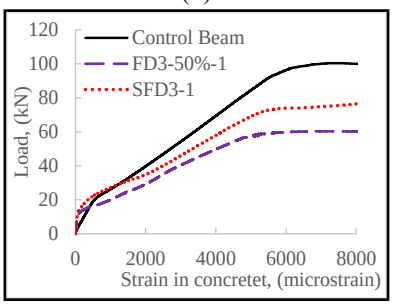

(c)

Fig. 9(a) Load displacement curves, (b) strain in reinforcement, (c) strain in concrete of control, flexural deficient (FD3) and CFRP strengthened (SFD3) RC beams

Table 3 Behaviour of deficient RC beams strengthened with one CFRP layer

Specimen ID	At yielding		At ultimate			D_R	Energy absorption (E) (kN mm)		
	P_y (kN)	δ_y (mm)	Load, Pu (kN) P_{ui}	Load, Pu (kN) P_{ua}	δ_u (mm)	$(\frac{\delta u}{\delta y})$	E_i	E_a	% Reduction
Control-0%-1	93.63	7.35	97.62		15.46	2.10	3174		
Control-0%-2	96.54	7.62	101.74	102	16.15	2.12	3477	3466	-
Control-0%-3	100.12	7.84	105.36		16.36	2.08	3748		
SFD1-1	96.20	7.26	108.12	107	12.62	1.73	3288	3211	7.35
SFD1-2	98.35	7.48	106.56		10.89	1.46	3134		
SFD2-1	94.55	7.62	104.54	105	13.36	1.75	2997	3059	11.72
SFD2-2	96.12	7.83	106.62		12.35	1.57	3122		
SFD3-1	73.12	5.94	85.17	84	9.10	1.53	1961	2009	42.03
SFD3-2	74.52	6.66	83.57		10.06	1.51	2058		

flexural deficient specimen -FD3 strengthened with more than one layer of CFRP fabric.

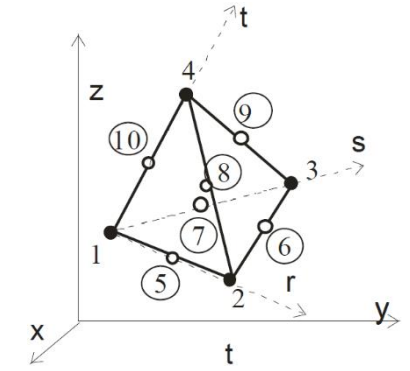

(a)

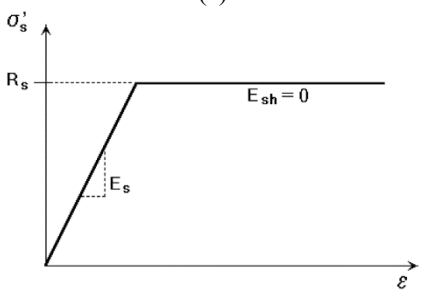

(b)

Fig. 10(a) Geometry of tetrahedral finite elements and (b) the bi-linear stress-strain law for reinforcement

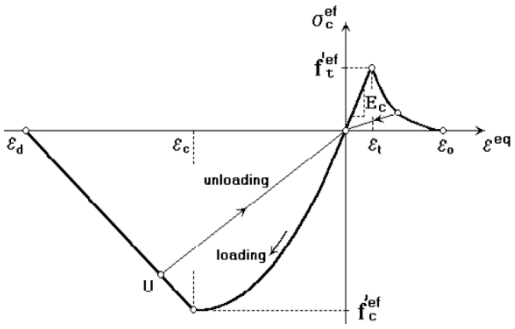

(a)

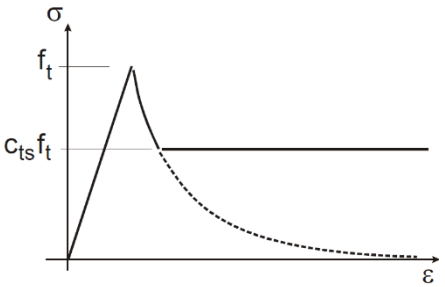

(b)

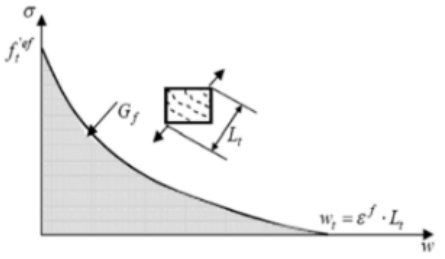

(c)

Fig. 11(a) Uniaxial constitutive law for concrete, (b) tension stiffening and (c) tensile softening and characteristic length

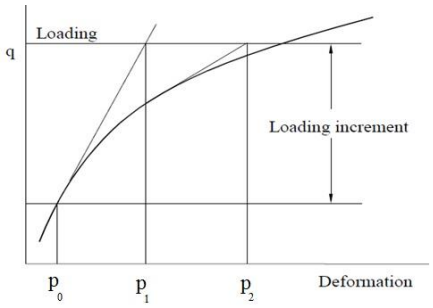

Fig. 12 Full Newton-Raphson method

5. Numerical investigations on flexural deficient (FD) and CFRP strengthened flexural deficient (SFD) RC beams

Numerical investigations are carried out on control, flexural deficient (FD3) and CFRP strengthened flexural deficient (SFD3) RC beams using commercial finite element analysis software ATENA. 3D nonlinear cementitious material and tetrahedral elements with 4 to 10 nodes as shown in Fig. 10(a) are used for modelling of concrete. These are isoperimetric elements and defined by at least four corner nodes. In this study, reinforcements are modelled as discrete bars and the bilinear stress-strain law as shown in Fig. 10(b) is assumed for all the reinforcements. The nonlinear behavior of concrete in the biaxial stress state is described by effective stress σ_c^{ef} and the equivalent uniaxial strain, ε^{eq}. The complete equivalent uniaxial stress-strain and tension stiffening adopted for concrete are shown in Figs. 11(a) and 11(b). Bazant and Oh (1983) proposed the characteristic length as a crack band size. In ATENA, crack band size L_t is calculated as a size of the element projection in the crack direction (as shown in Fig. 11(c)).

The load is applied in steps/increments as required by Newton Raphson method, in order to predict the nonlinear behaviour. Newton-Raphson method is an iterative process of solving nonlinear equations as shown in Fig. 12.

The stiffness matrix and vector of restoring loads are calculated on the basis of the displacement vector as given in Eq. (8).

$$K(\overline{p})\Delta\overline{p} = \overline{q} - f(\overline{p}) \tag{8}$$

where $\overline{q}$ is the vector of total applied joint loads, $f(\overline{p})$ is the vector of internal joint forces, $\Delta\overline{p}$ is the deformation increment due to loading increment, $\overline{p}$ are the deformations of structure prior to load increment, $K(\overline{p})$ is the stiffness matrix, relating loading increments to deformation increments.

For modelling de-bonding, stress based (perfect/ interfacial bond) and fracture mechanics based (cohesive zone modelling) criteria were reported in literature.

5.1 Stress based criteria

The perfect or interfacial bond between the composite and concrete was adopted by researchers (Nitereka and Neale 1999, Sasmal *et al.* 2013, Mostafa *et al.* 2013, Abu-Obeidah *et al.* 2015, and Banjara and Ramanjaneyulu 2017) for carrying out simulation studies on nonlinear behaviour of RC beams strengthened with FRP. Ebead and Marzouk (2005) proposed tensioning stiffening model to study the effect of FRP strengthening on ultimate load capacity of slabs. Even though these studies addressed complete load displacement behaviour and carrying capacity, de-bonding failure modes were not addressed.

5.2 Cohesive zone modelling (CZM)

In CZM modelling, the surfaces of cohesive zone ahead of crack tip are held by cohesive tractions (Jin and Sun 2005, Godat *et al.* 2012 and Sajedi *et al.* 2012). Cohesive traction is a function of the relative displacement of the top and bottom surfaces of 2D or 3D interface elements. The relative displacement is expressed in terms of the separation between the centres of the top and bottom faces of interface element. Wong and Vecchio (2003) and Lu *et al.* (2007) used interface elements between FRP and concrete in their studies. Park *et al.* (2015) investigated the interfacial debonding between FRP and concrete. Kim *et al.* (2015) used interfacial shear stress between FRP and concrete to evaluate the moment capacity of RC beams strengthened with FRP.

5.3 Numerical simulations for performance evaluation of CFRP strengthened deficient RC beams

Numerical simulations are carried out on control, flexural deficient (FD3) RC beams; and flexural deficient RC beam strengthened with one layer of CFRP fabric (SFD3). Finite element modelling of concrete and reinforcements of RC beams are modelled as shown in Figs. 13(a) and 13(b). Material properties such as modulus of elasticity (31,500 MPa), tensile strength (3.2 MPa), compressive strength (44.7 MPa) and fracture energy (126 N/m) for concrete are obtained based on the tests carried out in the present study and are assigned accordingly. Also, properties of reinforcement bar (Fe500), such as modulus of elasticity (200×10^3 MPa) and Poisson's ratio (0.3), of main reinforcements of beam bottom and top, shear reinforcement and steel plates are assigned appropriately. After that simply supported boundary conditions at the ends and loads at 1/3rd span points from both ends of the beam are applied. Monitoring points are defined at the locations where loads are applied and displacement responses are to be recorded. Fig. 13(c) shows macro element model of the RC beam with loading and reaction points and Fig. 13(d) shows finite element model of RC beam strengthened using CFRP fabric (SFD3).

CFRP is modelled as 2D (quadrilateral) membrane elements with composite material to capture orthotropic behavior. Epoxy resin is modelled as matrix and CFRP fabric is modelled as a smeared reinforcement. By specifying smeared reinforcement only in one direction (i.e., fibre direction), orthotropy is included in the model. This modelling requires input for the parameters of epoxy resin (matrix); namely, Young's modulus, Poisson's ratio, tensile strength, compressive strength, etc. The modelling also requires input for the parameters of CFRP fabric

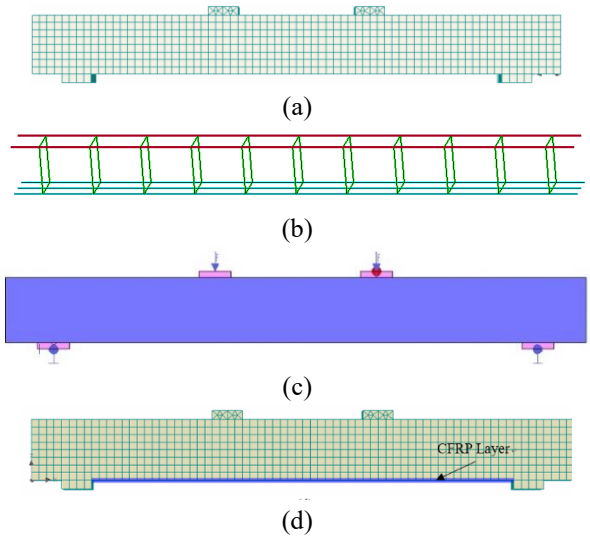

Fig. 13(a) Numerical model, (b) reinforcement details, (c) model with loading and reactions and (d) FE model of CFRP strengthened beam

(reinforcement); namely, Young's modulus, reinforcing ratio, direction of reinforcement and yield strength. The properties of CFRP material used in modelling are presented in Table 2. The contact between epoxy resin reinforced with CFRP fabric and concrete beam is represented using interface properties based on Mohr-Coulomb criterion with tension cut off.

For modelling, accuracy and convergence of results depend on mesh density. Trial analyses are carried out by varying the mesh size in order to obtain the optimum mesh density. An optimum mesh size of 25 mm is adopted for numerical investigations in this study. After meshing of the numerical model, loading is applied in steps/increments as required by Newton-Raphson method.

In this study, interface material model is used to simulate contact between two materials viz., concrete and CFRP. The interface material is modelled based on Mohr-Coulomb criterion with tension cut-off. The constitutive relation for a general three-dimensional case is given in terms of tractions on interface planes and relative sliding and opening displacements as given in Eq. (9). Linear bond-slip relationship for the interface is assumed in both tangential and normal directions.

$$\begin{Bmatrix}\tau_1\\ \tau_2\\ \sigma\end{Bmatrix} = \begin{bmatrix}k_{tt} & 0 & 0\\ 0 & k_{tt} & 0\\ 0 & 0 & k_{nn}\end{bmatrix}\begin{Bmatrix}\Delta v_1\\ \Delta v_2\\ \Delta u\end{Bmatrix} \quad (9)$$

where (τ) is the shear stress and (σ) is the normal stress in x and y direction. Δv is relative displacement on surface, Δu is relative opening of contact, K_{nn} and K_{tt} denotes the initial elastic normal and shear stiffness, respectively.

The initial failure surface corresponds to Mohr-Coulomb condition with tension cut off as given in Eq. (10).

$$|\tau| \le c + \sigma.\varphi, \quad \sigma \le f_t \text{ and}$$
$$\tau = 0, \quad \sigma \ge f \quad (10)$$

where: c is cohesion, φ is coefficient of friction, f_t is tensile strength on surface.

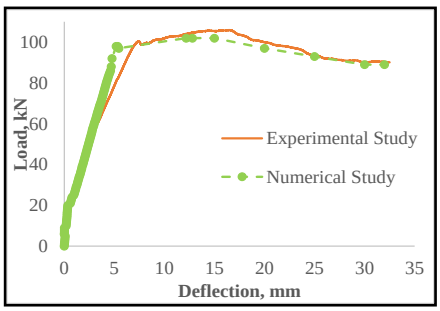

(a) Control beam

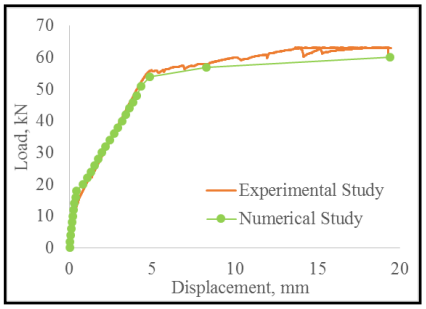

(b) FD3

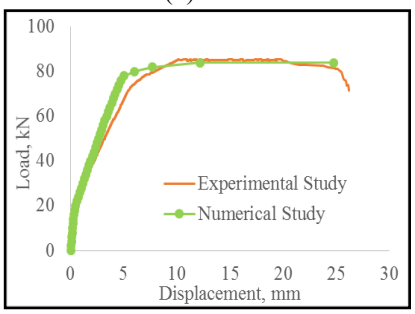

(c) SFD3

Fig. 14 Validation of (a) Control beam, (b) FD3 and (c) SFD3 with single layer of CFRP fabric

(a) Control beam (Experimental)

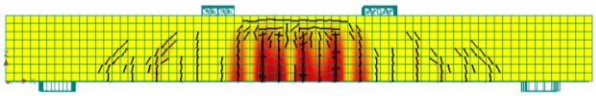

(b) Control beam (Numerical -crack width > 0.1 mm)

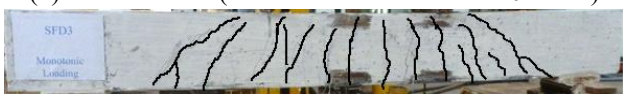

(c) SFD3 beam (Experimental)

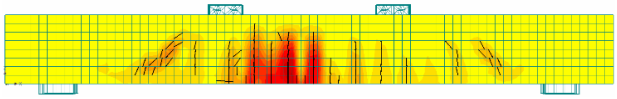

(d) SFD3 beam (Numerical -crack width > 0.1 mm)

Fig. 15 Crack formation in (a) control beam (experimental), (b) control beam (numerical), (c) SFD3 (experimental) and (d) SFD3 (Numerical)

Cohesion always has to be greater than (or at least equal to) tensile strength times the friction coefficient, i.e., $c \ge f_t\mu$.

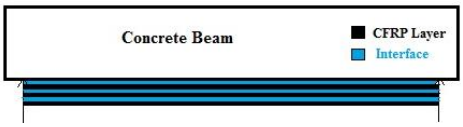

(a) Modelling of three layers of CFRP fabric

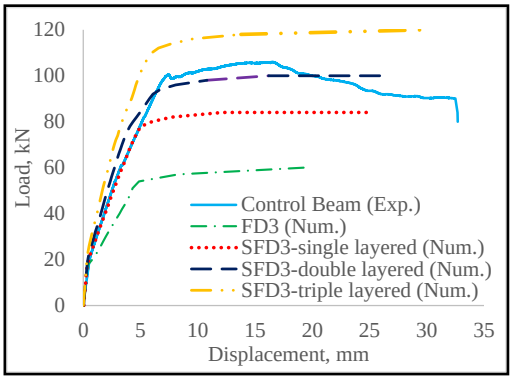

(b) Load versus displacement curves

Note: - Exp. - experimental investigations
Num. - numerical investigations

Fig. 16(a) Modelling of CFRP fabric layers and (b) Load displacement curves of control, FD3, SFD3 with single, double and triple layered CFRP fabric

Usually friction coefficient lies between 0.3-0.5. The value of friction coefficient between concrete surface and CFRP fabric is taken as 0.3.

The contact between concrete surface and CFRP fabric is considered as 3D interface having zero gap. To estimate the stiffness values of K_{nn} and K_{tt}, Eq. (11) is used.

$$K_{nn} = \frac{E}{t}, \qquad K_{tt} = \frac{G}{t} \tag{11}$$

where 'E' and 'G' is minimal elastic modulus and shear modulus respectively of the surrounding material such as concrete and 't' is the thickness of interfacial zone (epoxy) which is uses as 1 mm in this study. In numerical analysis, based on Eq. (11), K_{nn} and K_{tt} are used as 0.32×10^8 MN/m^3 and 0.13×10^8 MN/m^3 respectively.

6. Results and discussion

Finite element results of control, flexural deficient (FD3) and CFRP strengthened flexural deficient (SFD3) beams are compared with the experimental results as shown in Figs. 14(a)-(c), respectively. From this comparison, it is noted that the numerical simulation results, viz., load carrying capacity versus deflection of the RC beams are found to be within ±5% variation with respect to the results of experimental study.

From the results of finite element analysis, it is possible to visualize the cracks of smaller width which cannot be seen by naked eye. It is also possible to visualize the cracks greater than the specified crack width. The crack formation in control and CFRP strengthened critical flexural deficient RC beam (SFD3) with single layer of CFRP fabric from experimental and numerical investigations are shown in Figs. 15(a)-15(d), respectively. Figs. 15(b) and (d) show cracks of width greater than 0.1 mm.

From the results of the investigations, it is observed that one layer of CFRP fabric is not adequate to bring the load carrying capacity of critical flexural deficient RC beam (FD3) on par with that of control beam. Hence, for further numerical study, two and three number of CFRP layers are provided for strengthening of deficient RC beams. Modelling of three number of CFRP fabric layers used for strengthening of deficient RC beam is shown in Fig. 16(a). Interface models are used between the layers (same values of K_{nn} and K_{tt}) and simulations are carried out under monotonic loading. It is found that load carrying capacity of strengthened RC beam with two CFRP fabric layers has reached the load level equivalent to that of the control beam. With three layers of CFRP fabric, the load carrying capacity of strengthened RC beam has exceeded that of the control beam, as shown in Fig. 16(b). Hence, from the study, it is observed that two layers of CFRP fabric are sufficient to strengthen the critical flexural deficient RC beam -FD3. The numerical approach provides the means of evaluating the performance of CFRP strengthened deficient RC beams.

7. Conclusions

Experimental investigations on control, flexural deficient with three levels of deficiency are carried out under monotonic loading. It is found that load carrying capacity of 50% flexural deficient RC beam (FD3) is around 40% less than that of control beam. Hence, to improve the load carrying capacity of flexural deficient RC beams, CFRP fabric is used for strengthening. Analytical formulations are presented for designing number of layers of CFRP fabric required for strengthening.

It is found that one layer of CFRP fabric has improved load carrying capacity of FD1 (20% deficient) and FD2 (30% deficient) and their load carrying capacities after strengthening are found to be on par with that of the control beam. But, one layer of CFRP fabric has improved load carrying capacity of critical flexural deficient (50% deficient) RC beam (FD3) by 37% only and that is not sufficient enough to reach that of control specimen.

Hence, further investigations are carried out to improve the load carrying capacity of critical flexural deficient RC beam (FD3) through numerical simulations. Numerical investigations on control, critical flexural deficient (FD3) beams and critical flexural deficient RC beam strengthened with single, double and triple layered CFRP fabric (SFD3) are carried out. Interface between concrete and CFRP layers is modelled. It is found that CFRP fabric with single layer and double layers has improved the load carrying capacity of flexural deficient RC beam -FD3 approximately by 37% and 62%, respectively. The load carrying capacity of strengthened RC beam –SFD3 with two layers of CFRP fabric has reached the load capacity equivalent to that of the control beam. When three layers of CFRP fabric are used for strengthening, load carrying capacity of strengthened beam SFD3 exceeded the load carrying capacity of control beam. Hence, two layers of CFRP are found to be optimum for strengthening of the critical flexural deficient RC beam-

FD3. The validated numerical models and approach presented in this study can be adopted for evaluating the performance of deficient and CFRP strengthened RC beams.

Acknowledgments

Authors express acknowledgements to Dr. Saptarshi Sasmal, Dr. V. Srinivas and members of Structural Testing Laboratory at CSIR-Structural Engineering Research Centre for the help and support during the study.

References

Abu-Obeidah, A., Hawileh, R.A. and Abdalla, J.A. (2015), "Finite element analysis of strengthened RC beams in shear with aluminum plates", *Comput. Struct.*, **147**, 36-46.

ACI 440.2R-08 (2008), *Guide for the Design and Construction of Externally Bonded FRP Systems for Strengthening Concrete Structures*, ACI Committee 440, U.S.A.

Afefy, H.M., Sennah, K. and Akhlagh-Nejat, H. (2016), "Experimental and analytical investigations on the flexural behavior of CFRP-strengthened composite girders", *J. Constr. Steel Res.*, **120**, 94-105.

Ahmed, E., Sobuz, H.R. and Sutan, N.M. (2011), "Flexural performance of CFRP strengthened RC beams with different degrees of strengthening schemes", *Int. J. Phys. Sci.*, **6**(9), 2229-2238.

Banjara, N.K. and Ramanjaneyulu, K. (2017), "Experimental and numerical investigations on the performance evaluation of shear deficient and GFRP strengthened reinforced concrete beams", *Constr. Build. Mater.*, **137**, 520-534.

Bazant, Z.P. and Oh, B.H. (1983), "Crack band theory for fracture of concrete", *Mater. Struct.* RILEM, **16**(93), 155-177.

Bocciarelli, M., Feo, C.D., Nisticò, N., Pisani, M.A. and Poggi, C. (2013), "Failure of RC beams strengthened in bending with unconventionally arranged CFRP laminates", *Compos. Part B: Eng.*, **4**, 246-254.

Boukhezar, M., Samai, M.L., Mesbah, H.A. and Houari, H. (2013), "Flexural behaviour of reinforced low-strength concrete beams strengthened with CFRP plates", *Struct. Eng. Mech.*, **47**(6), 819-838.

Dias, S.J.E. and Barros, J.A.O. (2011), "Shear strengthening of RC T-section beams with low strength concrete using NSM CFRP laminates", *Cement Concrete Compos.*, **33**(2), 334-345.

Dong, J.F., Wang, Q.Y. and Guan, Z.W. (2012), "Structural behavior of RC beams externally strengthened with FRP sheets under fatigue and monotonic loading", *Eng. Struct.*, **41**, 24-33.

Ebead, U.A. and Marzouk, H. (2005), "Tension-stiffening model for FRP-strengthened RC concrete two-way slabs", *Mater. Struct.*, **38**(2), 193-200.

Ekenel, M., Rizzo, A., Myers, J.J. and Nanni, A. (2006), "Flexural fatigue behavior of reinforced concrete beams strengthened with FRP fabric and precured laminate systems", *J. Compos. Constr.*, **10**(5), 433-442.

El-Gamal, S.E., Al-Nuaimi, A., Al-Saidy, A. and Al-Lawati, A. (2016), "Efficiency of near surface mounted technique using fiber reinforced polymers for the flexural strengthening of RC beams", *Constr. Build. Mater.*, **118**, 52-62.

El-Zohairy, A., Salim, H., Shaaban, H., Mustafa, S. and El-Shihy, A. (2017), "Experimental and FE parametric study on continuous steel-concrete composite beams strengthened with CFRP laminates", *Constr. Build. Mater.*, **157**, 885-898.

Godat, A., Labossière, P. and Neale, K.W. (2012), "Numerical investigation of the parameters influencing the behaviour of FRP shear-strengthened beams", *Constr. Build. Mater.*, **32**, 90-98.

Grace, N.F., Sayed, G.A., Soliman, A.K. and Saleh, K.R. (1999), "Strengthening reinforced concrete beams using fiber reinforced polymer (FRP) laminates,", *ACI Struct. J.*, **96**(5), 865-874.

Haddad, R.H., Al-Rousan, R.Z. and Al-Sedyiri, B.K. (2013), "Repair of shear-deficient and sulfate-damaged reinforced concrete beams using FRP composites", *Eng. Struct.*, **56**, 228-238.

IS 456 (2000), *Plain and Reinforced Concrete*, Code of Practice, BIS, New Delhi, India.

Jin, Z.H. and Sun, C.T. (2005), "Cohesive zone modeling of interface fracture in elastic bi-materials", *Eng. Fract. Mech.*, **72**(12), 1805-1817.

Kim, N., Shin, Y.S., Choi, E. and Kim, H.S. (2015), "Relationships between interfacial shear stresses and moment capacities of RC beams strengthened with various types of FRP sheets", *Constr. Build. Mater.*, **93**, 1170-1179.

Lim, D.H. (2009), "Combinations of NSM and EB CFRP strips for flexural strengthening of concrete structures", *Mag. Concrete Res.*, **61**(8), 633-643.

Lu, X.Z., Teng, J.G., Ye, L.P. and Jiang, J.J. (2007), "Recent research on intermediate crack-induced debonding in FRP-strengthened RC beams", *J. Compos. Constr.*, **11**, 161-174.

Mostafa, E.M., Amr, E.R. and Ehab, E.S. (2013), "Experimental testing and finite element modeling on continuous concrete beams reinforced with fibre reinforced polymer bars and stirrups", *Can. J. Civil Eng.*, **40**(11), 1091-1102.

Nitereka, C. and Neale, K. W. (1999), "Analysis of reinforced concrete beams strengthened in flexure with composite laminates", *Can. J. Civ. Eng*, **26**(5), 646-654.

Park, K., Ha, K., Choi, H. and Lee, C. (2015), "Prediction of interfacial fracture between concrete and fiber reinforced polymer (FRP) by using cohesive zone modeling", *Cement Concrete Compos.*, **63**, 122-131.

Peng, H., Zhang, J., Shang, S., Liu, Y. and Cai, C.S. (2016), "Experimental study of flexural fatigue performance of reinforced concrete beams strengthened with prestressed CFRP plates", *Eng. Struct.*, **127**, 62-72.

Rusinowski, P. and Täljsten, B. (2009), "Intermediate crack induced debonding in concrete beams strengthened with CFRP plates-an experimental study", *Adv. Struct. Eng.*, **12**(6), 793-806.

Sajedi, S., Ghasemzadeh, F., Shekarchi, M. and Soleimani, M. (2012) "Numerical investigation on the effect of concrete-FRP bond on the flexural behavior of RC beams", *Proceedings of the Concrete Solutions, 4th International Conference on Concrete Repair*.

Saribiyik, A. and Caglar, N. (2016), "Flexural strengthening of RC Beams with low-strength concrete using GFRP and CFRP", *Struct. Eng. Mech.*, **58**(5), 825-845

Sasmal, S., Kalidoss, S. and Srinivas, V. (2013), "Nonlinear finite element analysis of FRP strengthened reinforced concrete beams", *J. Inst. Eng. Ind. Ser. A*, **93**(4), 241-249.

Wenwei, W. and Guo, L. (2006), "Experimental study and analysis of RC beams strengthened with CFRP laminates under sustaining load", *Int. J. Sol. Struct.*, **43**(6), 1372-1387.

Wong, R.S.Y. and Vecchio, F.J. (2003), "Toward modeling of reinforced concrete members with externally bonded fibre-reinforced polymer composites", *ACI Struct. J*, **100**(1), 47-55.

Yang, X., Gao, W-Y., Dai, J.G., Lu, Z.D. and Yu, K.Q. (2018),

"Flexural strengthening of RC beams with CFRP grid-reinforced ECC matrix", *Compos*. *Struct*., **189**, 9-26.
Zhang, W. and Kanakubo, T. (2016), "Flexural strengthening of RC beams with externally bonded CFRP plate: Experimental study on shear-peeling debonding", *Mag*. *Concrete Res*., **68**(14), 724-738.

CC